Flexural buckling of thin-walled channel members with slotted web: numerical and analytical studies

Dávid Visy, Máté Szedlák, Bori Geleji, Sándor Ádány

Budapest University of Technology and Economics
Department of Structural Mechanics
1111 Budapest, Műegyetem rkp. 3, Hungary,
e-mail: sadany@epito.bme.hu

Abstract

In this paper elastic major-axis flexural buckling of thin-walled channel members with slotted webs is discussed. First the behaviour is studied, and the major influencing factors are identified by using the recently developed constrained finite element method, which makes it possible to separate the behaviour/buckling modes, as well as provides with full control on the details of the calculations. It is found that, though other factors have some influence on the buckling results, the most important factor is the in-plane shear deformations of the slotted web, which can be disregarded, partially, or fully considered. The existence of these influencing factors highlights the importance of a proper definition for flexural buckling. An analytical model is also proposed for the calculation of critical force of slotted-web members, which model is able to consider the effect of shear deformations, the degrading effect of the slots on the axial and bending rigidity, as well as the effect of longitudinal second-order strain terms (which is included in typical shell models, but disregarded in most beam models). Extended numerical studies have been conducted, covering a wide range of column lengths and slot geometries. The results of the numerical studies justify the applicability of the constrained finite element method, as well as show that the analytical model estimates the critical loads with reasonably accuracy.

1 Introduction

Cold-formed steel members sometimes have holes due to various reasons and in various arrangements. There might be few larger openings, as well as many smaller holes. A special version of this latter case is when the profile, typically channel member, is produced with slotted web. Though the introduction of slots is in order to improve heat transfer characteristics, i.e., slots are applied due to non-structural reasons, they have non-negligible influence on the structural behaviour, too.

When a thin-walled member is subjected to compressive actions, buckling has pronounced role in the behaviour. It is typical to distinguish in between global (G), distortional, (D), local (L), in-plane shear (S) and transverse extension (T) deformation modes. Classic buckling modes can easily be assigned to the various deformations modes: global buckling (such as flexural or flexural-torsional buckling of columns, or lateral-torsional buckling of beams) is characterized primarily by G deformations, distortional buckling by D deformations, and local buckling (e.g., local-plate buckling, shear buckling, web crippling) by L deformations. However, S and T deformations sometimes have significance, too; in this paper the important effect of in-plane shear will be discussed in detail.

The buckling behaviour is, in general, complex, and the introduction of holes further increases the complexity. During the last few decades cold-formed steel members with holes have been studied by several research projects. Many publications are discussing elastic stability problem, see e.g. [1-4]. Others are aiming to study the nonlinear behaviour, either by performing real experiments or advanced numerical analysis, see e.g. [5-10]. Numerical methods have also been proposed specifically for the analysis of thin-walled members with holes, especially when smaller holes are present in a regular distribution, such as in rack uprights [11-12]. Similarly, in [13-15] an approximate method is proposed for member with holes, by using reduced thickness to account for the effect of holes.

All these approaches cannot formally perform modal decomposition, i.e., cannot formally separate the behaviour into G, D, L, modes. Since our purpose here is to study one specific type of buckling, separation of the buckling types is essential. There are two well-known methods for the separation of behaviour modes, namely: the generalized beam theory (e.g., [16-17]) and constrained finite strip method (e.g. [18-22]). Originally none of these methods could handle members with holes, later, however, the methods or the underlying concept have evolved into methods that can (at least partially) separate the behaviour modes, see e.g. [23-28]. None of these proposals, however, is general enough.

In this paper a general-purpose commercial finite element software (Ansys, [29]) and the so-called constrained finite element method (cFEM) are applied. In Ansys formal decomposition is not possible in general. On the other hand, cFEM is designed with the ability of formal separation of behaviour modes, see [30-33]. cFEM is essentially a shell finite element method, therefore can easily handle members with holes, as already discussed in [34]. Therefore, cFEM is an ideal candidate for the analysis of slotted cold-formed steel members.

Though thin-walled members with holes are extensively, members with slotted webs are much less discussed by research papers. Some papers are focusing on the thermal properties (which is out of the area of this actual paper), while other on the strength properties. Research on the mechanical behaviour of members with slotted webs started (most probably) in the beginning of the 90's, the first results summarized in (not-easily accessible) research reports. In [35] there is an overview of these first results, describing the characteristic behaviour of studs with slotted web, identifying the specialities of the behaviour (e.g., radically reduced shear rigidity of the slotted web). In [36] and experimental program is reported on steel partition walls, mostly non-slotted members are tested, but slotted stud is considered, too. [37] is focusing on slotted plates (rather than members with slotted web), on the basis of results of nonlinear FE analyses design equations are proposed for local buckling (employing effective width method). Lately, Degtyareva and Degtyarev published papers [38-42] on the shear behaviour of channel members with slotted web, including experimental results, elastic and nonlinear finite element simulations, as well as proposals for design against shear buckling. In [43] there is a review on the bending behaviour of channel members with slotted web.

The available publications are focusing on the local behaviour of the slotted webs, either local-plate buckling or shear buckling, but no detailed results are found on the global behaviour. The authors of the actual paper reported some results on the flexural buckling of various slotted members in [44], which results now are significantly extended, by utilizing the abilities of the recently proposed cFEM. In this paper major-axis buckling is discussed only. It is to note that while major-axis flexural buckling is a natural buckling mode for double-symmetrical cross-sections, it is not a natural buckling mode for mono-symmetric channel members. If the member is not specifically supported, it would buckle in minor-axis flexural mode or in flexural-torsional mode. However, if torsion of the member is prevented, major-axis flexural mode becomes realistic. Since the channel members with slotted webs are frequently supported laterally by an adjoining component (e.g., by some OSB, gypsum board or trapezoidal sheeting), it is reasonable to consider major-axis buckling. In this paper, therefore, major-axis

(elastic) flexural buckling is discussed only. The effect of slotted web is investigated numerically, by using shell finite element analysis (Ansys and cFEM). The major factors that influence the behaviour are identified, with a special focus on the effect of in-plane shear deformations which is found to be a crucial factor. An analytical model is also proposed for the calculation of flexural buckling of channel columns with slotted web. The influence of the parameters of the model is discussed in detail, as well as the results are compared to results of shell finite element calculations.

2 Slotted members and numerical models

2.1 Slotted channel members

To analyse the effect of holes, numerical and analytical studies have been performed. Column members are analysed with and without slots. Various channel-like cross-sections are selected, C-shaped cross-sections, and channel sections with a pronounced web stiffener (centrally positioned in the web) called Sigma section. When slots are applied, they are centrally positioned in the web of the C-section, while two variations are considered for the Sigma-sections: (i) symmetrically positioned slots below and above the web stiffener (referred also as SS-section), or (ii) asymmetrically positioned slots, located only above or below the web stiffener (referred also as SA-section). The sections are illustrated in Fig. 1. The following dimensions are used: 200 mm for the web height, 40 mm for the flange widths, 20 mm for the lip lengths, and 2 mm for the thickness. The given dimensions are out-to-out dimensions. The lips are perpendicular to the flanges. In the case of SA/SS-sections the web stiffener has a height of 15 mm and width of 30 mm.
Members without holes and with slotted webs are considered In case of slotted webs the assumed slot pattern is shown in Fig. 2. During the studies the slot sizes and slot distances are kept constant, however, the number of slot rows is varying from 1 to maximum 15.

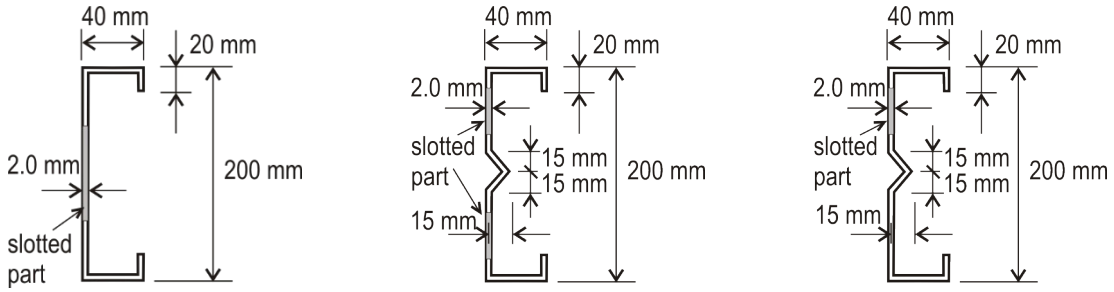

Figure 1: Channel section with/without web stiffener

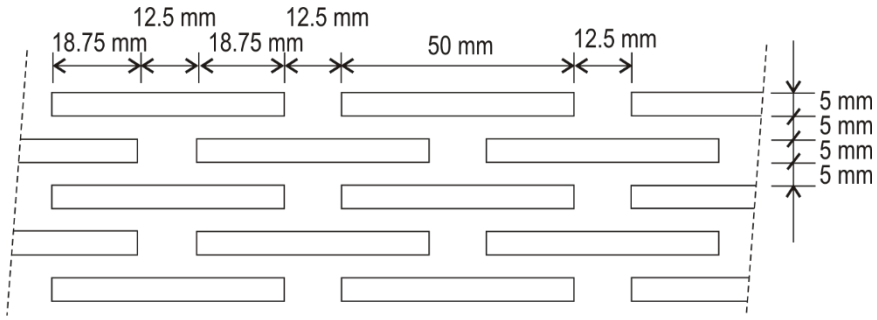

Figure 2: Slot pattern

The considered material has characteristics similar to regular steel. However, previous studies highlighted that when constraining is applied to prevent transverse deformations of the cross-sections, it introduces an increase of the axial stiffness (as well as all the stiffness parameters associated with warping), therefore, results are more realistic if the Possion's ratio is set to zero. (For more details, see [45]). Thus, the material properties are as follows: E = 210 000 MPa and ν=0.

Various column lengths are considered. In all the cases the column members have simple supports at both ends. Since the members are thin-walled, various buckling modes can be calculated by a regular shell FE analysis, including plate buckling and distortional buckling. Here, however, major-axis buckling modes are investigated, therefore, it was an aim to eliminate other buckling types from the analysis.

2.2 Commercial shell FE model

As a commercial finite element software, the Ansys software is used [29]. Thin shell elements are employed based on Kirchhoff plate theory, called SHELL63 in Ansys. Preliminary studies showed that the results are relatively sensitive to discretization, so a relatively fine mesh is necessary (e.g., with at least 2-3 elements transversally between the slot rows). The analysed column is simply-supported which means that the ends are free to rotate about the transverse axes and free to warp, but restrained against transverse translations and restrained against twisting rotation. The column is loaded by two concentrated longitudinal forces at its ends, equal in magnitude but opposite in direction, which is resulted a compressive axial force. The end forces are applied as distributed loads along the mid-lines of end cross-sections.

The analysed members are constrained in order to exclude other than global buckling modes. Two types of constraints are applied, as follows: (c1) constraints to exclude cross-section deformations, (c2) constraints to exclude in-plane shear deformations. If c1+c2 constraints are used, this leads to classical shear-free bending deformations. If c1 is used without c2, this leads to global modes with in-plane shear. The constraints are realized as follows. Criterion c1 is enforced by introducing 'virtual diaphragms'. Virtual diaphragm ensures that transverse displacements (i.e., transverse translations and rotation about the column's longitudinal axis) in a cross-section are linked to each other. (In Ansys this kind of constraint can readily be realized by the CERIG command.) Criterion c2 means the exclusion of in-plane (membrane) shear deformations of the plate elements of the cross-section. A straightforward way to realize it in an Ansys FE analysis is to apply a special finite element (called SHELL28) with increased shear rigidity. Note, some more details on how to do the constraining in Ansys can be found in [45].

2.3 cFEM model

Constrained finite element method (cFEM) is essentially a shell finite element calculation, but the method is developed so that modal decomposition would be possible. Separation of the behavior modes is realized by applying mechanical constraints. In order to maintain constraining ability, the longitudinal shape functions are specially selected, but the shell elements can be used as any regular flat shell element.

When a member is constrained into G, D, L, etc. deformation mode, it is enforced to deform in accordance with some mechanical criteria, characterizing for the intended deformation mode. These criteria are formulated by displacements and displacement derivatives (i.e., strains). The

criteria can be expressed by constraint matrices that are denoted, in general, by **R**. The application of the constraint matrix enforces to fulfil certain relationship between various nodal degrees of freedom, specific to the given 'M' deformation space. This automatically means a reduction of the effective degrees of freedom. Mathematically, the **d** displacement vector is expressed as follows:

$$d = R_M d_M \tag{1}$$

where $\mathbf{R_M}$ is a so-called constraint matrix to the M space, and $\mathbf{d_M}$ is the reduced displacement vector. Since the $\mathbf{d_M}$ reduced displacement vector has fewer elements than that of the original **d** vector, the elements of $\mathbf{d_M}$ vector cannot (typically) be interpreted as nodal displacements anymore. Another view of the above expression is therefore: the column vectors of the constraint matrix are the *base vectors* of the displacement field that is represented by the constraint matrix, and the **d** displacement vector is expressed as a linear combination of base vectors and combination factors, which latter ones are nothing else than the elements of the $\mathbf{d_M}$ vector. 'M' might be G, D, L, S or T, or, in fact, 'M' might mean any combination of base vectors from any spaces.

By using the constraint matrix, solution in a reduced, specific deformation space is possible. For example, first-order static analysis can be done. In this case the (unconstrained) problem has the following form:

$$K_e d = f \tag{2}$$

where $\mathbf{K_e}$ is the (elastic) stiffness matrix, **d** is the displacement vector and **f** is the load vector. If deformations are constrained, the problem can be written as follows:

$$K_e R_M d_M = f \tag{3}$$

from which

$$R_M{}^T K_e R_M d_M = R_M{}^T f \tag{4}$$

$$K_{eM} d_M = f_M \tag{5}$$

where $\mathbf{K_{eM}}$ and $\mathbf{f_M}$ can be regarded as the modal version of the stiffness matrix and load vector, respectively, constrained into the given 'M' deformation space.

In case of linear buckling analysis the problem is formulated mathematically as a generalized eigen-value problem, namely:

$$K_e \Phi - \Lambda K_g \Phi = 0 \tag{6}$$

where $\mathbf{K_e}$ and $\mathbf{K_g}$ are the global elastic and geometric stiffness matrices, and

$$\Lambda = diag<\lambda_1 \lambda_2 \lambda_3 \ldots \lambda_{nDOF}> ¿ \Phi = [\phi_1 \phi_2 \phi_3 \ldots \phi_{nDOF}] \tag{7}$$

where λ_i is the critical load multiplier and ϕ_i is the associated buckling shape, and *nDOF* denotes the number of degrees of freedom.

When the constraints are enforced, the displacement vector is expressed by modal coordinates, see Eq. (1). This equation can also be applied to any buckling shape ϕ, since the buckling shape itself is a displacement vector. Therefore:

$$\phi = R_M \phi_M \tag{8}$$

By substituting Eq. (8) to Eq. (6), then multiplying (from the left) by the transpose of the constraint matrix, the eigen-value problem can be written as:

$$R_M{}^T K_e R_M \Phi_M - \Lambda_M R_M{}^T K_g R_M \Phi_M = 0 \tag{9}$$

which is another generalized eigen-value problem, given in the reduced M deformation space:

$$K_{eM} \Phi_M - \Lambda_M K_{gM} \Phi_M = 0 \tag{1}$$

Solving the above equation leads to the modal eigen-vectors, from which the buckled shapes can be back-calculated by using Eq. (8).

3 Flexural buckling of a slotted column

3.1 General

Flexural buckling is probably the simplest form of buckling, when an initially straight column under the effect of a sufficiently big concentric compressive force is suddenly subjected to significant lateral displacements (but the displacements take place in a single plane, without any twist of the member). Though some solution for the critical force exists for more than 200 years, and though this type of buckling is taught in undergraduate classes, the exact definition of flexural buckling is not obvious in slightly more complicated cases such as a thin-walled column member with web slots.

It can be considered as universally agreed that the notion of flexural buckling is usually interpreted in the realm of beam/column members, i.e., when the member can reasonably be modelled by a beam-model. Consequently, flexural buckling assumes the lack of any significant cross-section deformation. This alone, however, does not define the buckling shape unambiguously.

In some cases the proper calculation of the critical load is not possible by using beam-models. A characteristic example is a thin-walled member (especially if holes are present). Thin-walled members can conveniently be modelled by shell-models, such as finite strip model or finite element with using (flat) shell elements. If shell-model is used, however, flexural-buckling-like buckled shape can be achieved by various ways, but sometimes with significantly different critical load values.

3.2 Second-order strains, through-thickness distribution

In [46] global column buckling of thin-walled members is discussed, including flexural buckling. The discussion is based on shell model. A possible definition is also given if in-plane shear deformations in the plate elements is excluded, which lead to analytical solution similar or identical to the classical global column buckling formulae. Three major aspects have been revealed: the Poisson-effect, the effect of selection of second-order strain terms, and whether the variation of strain/stress through the plate thickness is considered or disregarded.

If cross-section deformations are fully restrained, as suggested by beam-model, the restrained transverse extensions/contractions in the shell models lead to a virtual increase of axial rigidity, hence to a difference between shell-model-based and classical buckling solutions. The difference is dependent on the Poisson's ratio and the type of buckling, and disappears if Poisson's ratio is (forced to be) zero.

It has moreover been shown that the longitudinal second-order strain term (from the Green-Lagrange strain matrix) has important effect on the results, especially for (very) short columns. In classical solutions, as in a typical beam-model approach, this longitudinal second-order strain term is disregarded, but in case of typical (numerical) shell models it is considered, which has also been demonstrated by various numerical calculations in [45].

In [46] it has also been shown that some, typically small, variation of the calculated critical load is due to the considered or disregarded variation of the strains/stresses through the plate thickness.

These factors have certain effect on the critical loads for any thin-walled member. However, if holes are present, further factors might influence the behaviour. These factors have partially been discussed in [43], and comprehensively discussed as follows.

3.3 Rigidity degradation due to removed material

An obvious effect of the presence of the removed material is that they reduce the flexural rigidity of the beam. In case of slotted webs the reduction is certainly dependent on the slot pattern, namely on how many slot rows we apply, and also on the size and arrangement of slots. Supposedly, the rigidity reduction is not constant along the length, since the amount of the removed material is dependent on the location of the cross-section. There are three typical cross-sections, as illustrated in Fig. 3 (for 5 slot rows).

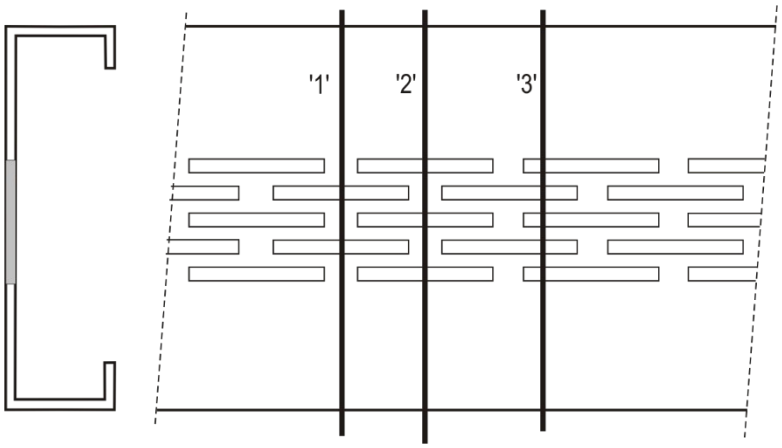

Figure 3: Reduced cross-sections due to slotted web

The rigidity degradation is demonstrated here in two ways. In Tables 1-3 the moment of inertias are given for the considered cross-sections, depending on the number of slot rows. As the numerical values prove, the reduction of the moment of inertia is non-negligible.

Table 1: Reduction of the moment of inertia due to slots, C section

nr or slot rows		0	3	7	11	15
inertia at 1	mm^4	3394600	3394579	3386538	3354496	3282454
inertia at 2	mm^4	3394600	3392558	3374517	3324475	3226433
inertia at 3	mm^4	3394600	3392538	3366454	3284371	3114288

Table 2: Reduction of the moment of inertia due to slots, SS section

nr or slot rows		0	3×2	5×2	7×2
inertia at 1	mm^4	3396478	3331456	3262435	3185413
inertia at 2	mm^4	3396478	3262435	3185413	3096391
inertia at 3	mm^4	3396478	3197413	3051370	2885326

Table 3: Reduction of the moment of inertia due to slots, SA section

nr or slot rows		0	3	5	7
inertia at 1	mm^4	3396478	3363459	3327390	3286221
inertia at 2	mm^4	3396478	3327390	3286221	3237897
inertia at 3	mm^4	3396478	3292221	3210361	3113399

In Fig. 4 the reduction of the critical force is plotted in the function of slot rows. The critical force values are calculated by cFEM, with forcing global flexural deformations. Various column lengths have been considered (between 300 and 5000 mm), but the reduction show very small scatter, so it can be concluded that the reduction of the critical force is independent of the column length. As Fig. 4 shows, the Sigma profiles are more affected by the slots, which is explained by the fact that in the Sigma sections the slots are located farther from the neutral axis. Moreover, the asymmetric placement of the slots slightly increases the critical force reduction.

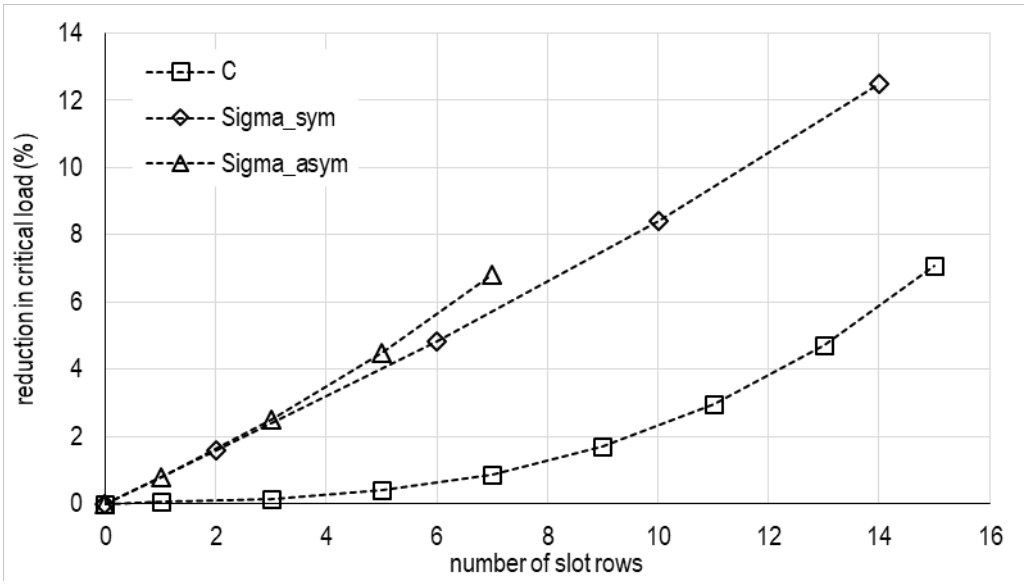

Figure 4: Critical load reduction due to removed material

3.4 The effect of shear deformations

It is known that the slots reduce the in-plane shear rigidity of the web plate. This reduction might have important effect on the flexural buckling critical load. There are at least three options how to consider the in-plane shear deformations: (a) totally exclude, (b) exclude in the steel material but allow in the holes, (c) allow in the steel material, too.

The difference between the three options can clearly be visualized by considering a channel member with a few large rectangular holes. The characteristic deformations are shown in Fig. 5.

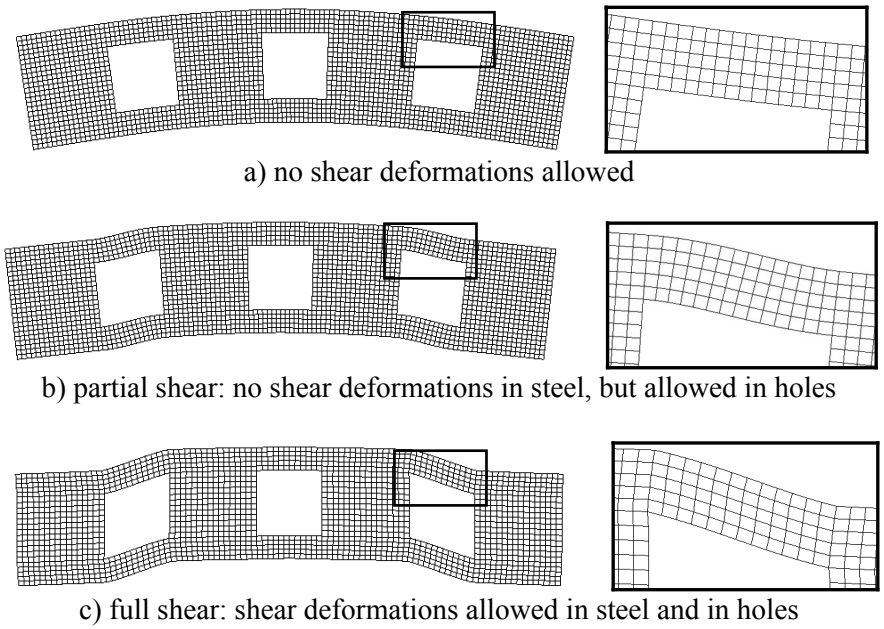

Figure 5: Characteristic deformations by neglecting or considering in-plane shear deformations

In case of slotted web the differences are less visible, but the effect of shear deformations is easy to observe by the critical load values. The critical load values are reduced due to the shear deformations, the reduction is plotted in Figs. 6-8.

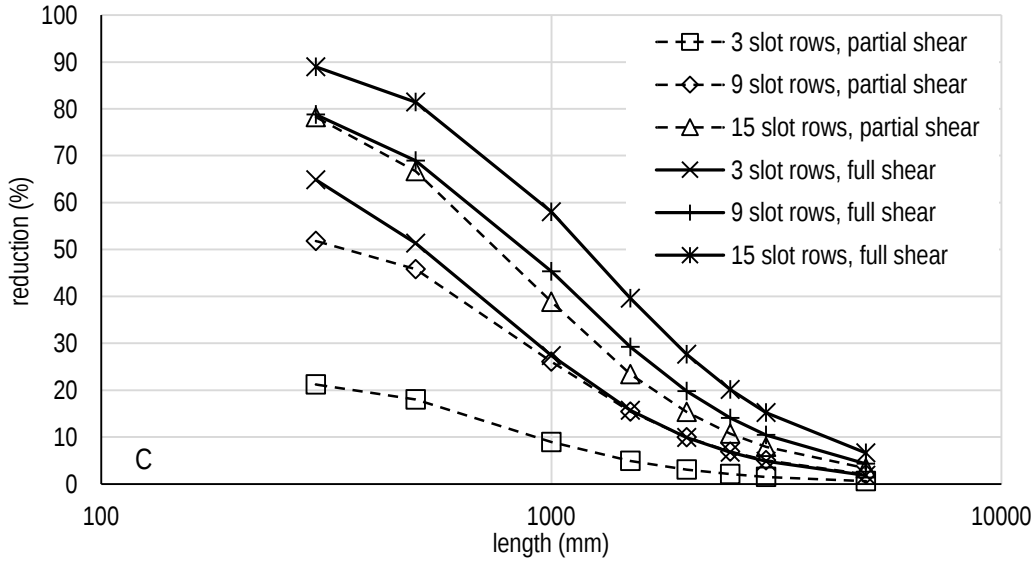

Figure 6: Critical load reduction due to shear deformations, C section

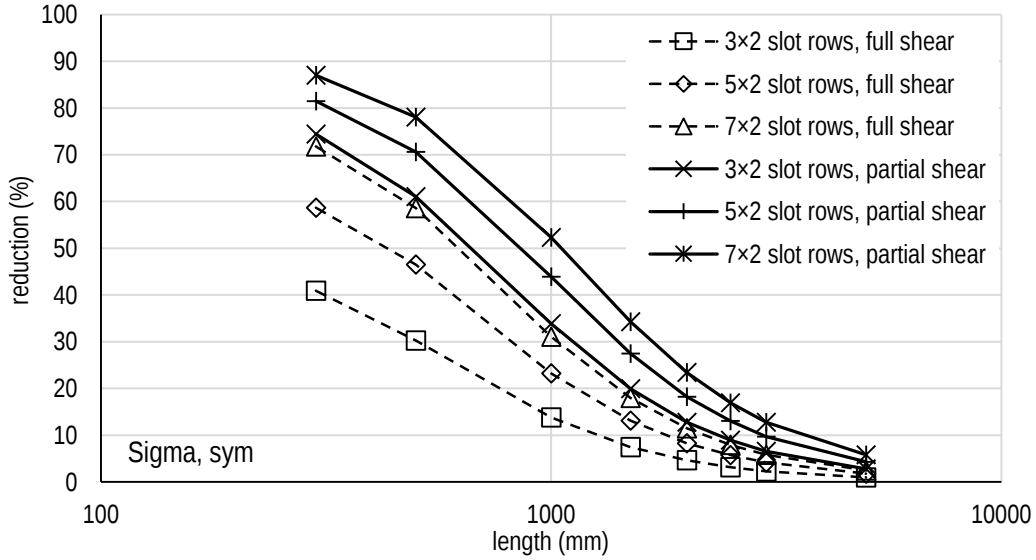

Figure 7: Critical load reduction due to shear deformations, SS section

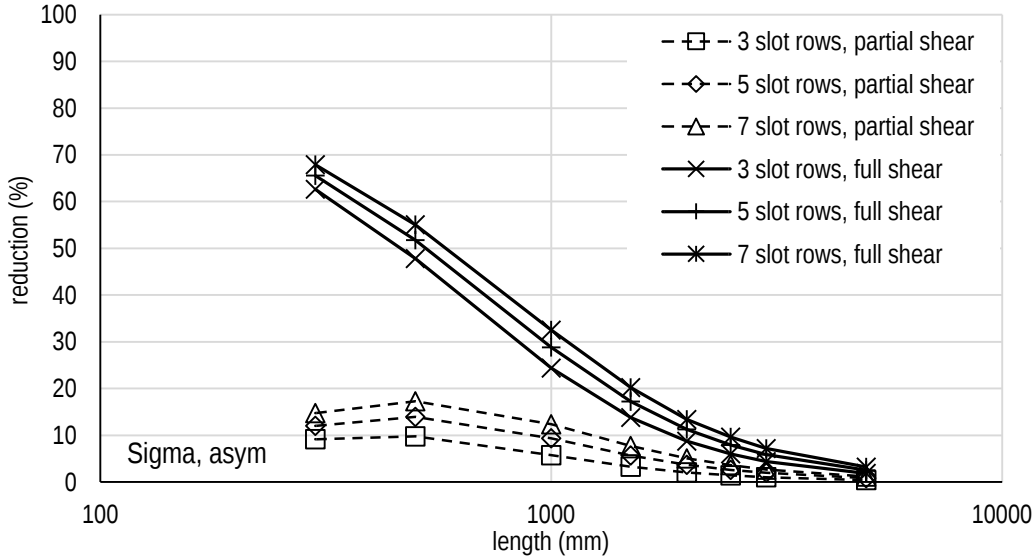

Figure 8: Critical load reduction due to shear deformations, SA section

There are tendencies that are common in all the three sections, namely: (i) the effect of shear deformations is decreasing with the increasing of the length, (ii) the effect of shear deformations is increasing with the number of slot rows, and (iii) 'full shear' leads to larger reduction compared to 'partial shear'.

There are differences in the tendencies depending on the cross-section. It seems that the web stiffener itself does not significantly modify the tendencies, but the asymmetry of the slot pattern does, that is why the results of SA are different from those of C and SS.

It is to understand that 'partial shear' option is a possible generalization of the classic beam-model-based assumptions for global buckling, since classic solutions assume no in-plane shear deformations in the material, i.e, in the plates from which the thin-walled member is built up. Evidently, 'partial shear' option converges to classical solution as soon as the number of holes converges to zero. But even in this option the reduction of critical force is at least a few percentage, and can be as large as 10-20%, depending on the column length and the number of slot rows. And this reduction is added to the few percent reduction due to the flexural rigidity reduction caused by the removed material.

3.5 The effect of initial stress state

If shell finite element model is employed to calculate flexural (i.e., global) buckling, it is necessary to eliminate any (significant) deformation of the cross-sections. In case of a commercial FEM package this is not an easy task. In Ansys, as described in Section 2.2. rigid constraints can be defined, by the application of which diaphragms can be formed at multiple cross-sections, so that the cross-section deformations are (practically) eliminated. In order to have buckling solution, an initial stress state is necessary from which the geometric (or stress) stiffness matrix can be calculated. In a shell finite element calculation the initial stress state is determined by a first-order linear static analysis. It is to observe that in case of the actual Ansys calculation the rigid diaphragms have effect not only on the buckled shapes, but also on the first-order deformations, hence, on the first-order stress state. In other words, in case of the Ansys calculations the initial stress state is determined by a constrained shell model.

The cFEM method provides with a more general, and practically simpler way, since in cFEM any modal deformation can easily be enforced, including global deformations modes. For the actual cases, there are still two alternatives how the desired major-axis flexural buckling can be achieved. One way is to constrain the deformation into global modes. In this case we need to apply lateral supports for the member since otherwise there would be a minor-axis flexural and two flexural-torsional buckling modes instead of the intended major-axis flexural buckling. The other way to achieve major-axis flexural buckling is to constrain directly into major-axis flexural deformation mode. In that case there is no need to use lateral supports to avoid the lateral and torsional displacements. In the actual cFEM implementation it is optional whether the initial stress state is determined from constrained or unconstrained analysis. To demonstrate the effect of initial stress state, 3 options are compared here:

(a) the member is without lateral supports, the buckling is constrained to major-axis flexural mode, and the first-order analysis is unconstrained;

(b) the member is with lateral supports, the buckling is constrained to global modes, and the first-order analysis is unconstrained;

(c) the member is with lateral supports, the is buckling constrained to global modes, and the first-order analysis is constrained.

The first-order solutions are shown in Fig. 9, with magnifying the displacement by 10000. The colouring is in accordance with the longitudinal normal stresses.

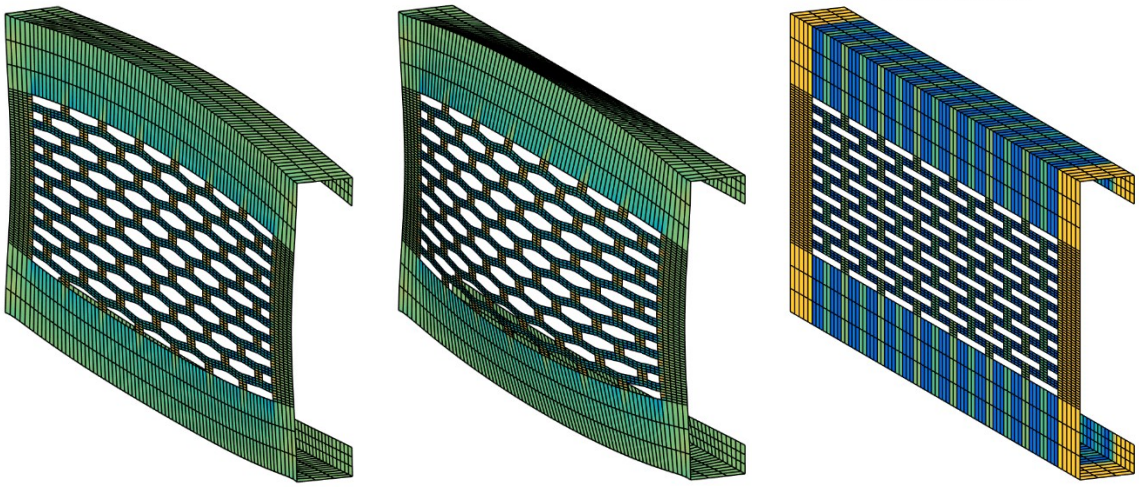

option (a):
without lateral supports,
unconstrained first-order

option (b):
with lateral supports,
unconstrained first-order

option (c):
with lateral supports,
constrained first-order

Figure 9: First-order longitudinal normal stresses, C section,

In option (a) the first-order displacements include some minor-axis bending, caused by the eccentricity of the loading, which is centric for the gross cross-section, but slightly eccentric in cross-sections with the slots. This eccentricity, however, is small; even though it makes the normal stress distribution slightly uneven in the flanges, this variation of normal stresses is very small. In option (b) the minor-axis bending is excluded by the applied lateral supports, which ensures a more constant stress distribution in the flanges, but still the stresses are very similar to those of option (a). In option (c) the cross-section deformations are effectively prevented, so the uniform stress distribution is enforced in each cross-section. This also means that the first-order stress is discontinuous along the length. This illustrates that constraining a first-order solution might lead to unexpected results, therefore requires special care.

Even though the first-order solutions have some distinct differences qualitatively, depending on the details of the supports and constraining, quantitatively the differences in the critical loads are fairly small. Between options (a) and (b) the differences are well below 1% for any of the analysed cases. The differences between options (c) and (a)/(b) are slightly larger, but still negligible for most of the cases. The maximum difference is sometimes larger than 1%, but only if the member is very short (i.e., 300-500 mm), if it has many slot rows, and if shear deformations are totally prevented. In all the other cases the difference caused by the initial stress state is practically negligible.

4 Analytical model for flexural buckling

4.1 Model without shear deformations

Classical shear-free flexural buckling (or: in general, global buckling) of columns with solid webs have been comprehensively studied in [45-46]. Various beam-like and shell-like models are considered, and analytical solutions are also derived in various options, including options that can (practically) precisely imitate constrained shell models such as the Ansys shell FE model used in this study. According to the referenced papers, the option that best fit to

constrained shell FEM is denoted there as ‘yny’, and the corresponding formula for flexural buckling is:

$$F_{cr}=\frac{1}{1-\nu^2}\frac{\pi^2 EAI}{L^2 A+\pi^2 I_r}=\frac{1}{\frac{1}{F_F}+\frac{1}{F_a}\frac{F_{Fr}}{F_F}} \tag{11}$$

where

$$F_F=\frac{\pi^2 EI}{(1-\nu^2)L^2} \tag{12}$$

$$F_{Fr}=\frac{\pi^2 E I_r}{(1-\nu^2)L^2} \tag{13}$$

$$F_a=\frac{EA}{1-\nu^2} \tag{14}$$

where E is the modulus of elasticity, ν is the Poisson’s ratio, L is the member length, while the involved cross-sectional properties are as follows: A is the cross-sectional area, I is the second moment of areas calculated for the relevant (e.g., strong) axis with considering own plate inertias (i.e., the (‘*width*’)×(‘*thickness*’)^3/12 terms), while I_r is the same second moment of area but with neglecting own plate inertias. In case of thin-walled members $I\simeq I_r$ hence $F_F\simeq F_{Fr}$, therefore the formula can approximately be written as:

$$F_{cr}\cong\frac{1}{1-\nu^2}\frac{\pi^2 EAI}{L^2 A+\pi^2 I}=\frac{1}{1/F_F+1/F_a} \tag{152}$$

Note, this formula is exactly identical to the one that belongs to ‘yyy’ option in [45-46].

As numerical results clearly show, the effect of holes is not negligible, even if the in-plane shear is neglected. The above formula can most surely be used, but with reduced section properties. Assuming that the web slots are present along the whole length of the member (which is the typical practical situation), it is reasonable to assume that an equivalent constant axial and bending stiffness can be defined. The equivalent section properties accounting for the slots are proposed to calculate as the weighted average from the characteristic cross-sections, as follows:

$$A_{eq}=\rho_1 A_1+\rho_2 A_2+\rho_3 A_3 \tag{3}$$

$$I_{eq}=\rho_1 I_1+\rho_2 I_2+\rho_3 I_3 \tag{4}$$

where A_1, A_2 and A_3 are cross-section areas with considering the holes due to the slots, while I_1, I_2 and I_3 are moment of inertias for the relevant (i.e. strong) axis calculated with considering the holes. The ‘1’, ‘2’ and ‘3’ locations are illustrated in Fig. 3. Obviously, the values of the ρ coefficients are dependent on the arrangement of the slots. Evidently, $\rho_1+\rho_2+\rho_3=1$, and it is reasonable to assume that ρ_1 should be equal to ρ_2 (in case of any regular slot arrangement), while ρ_3 should have the largest value out of the three. The simplest approach to get the ρ values is to calculate the total (relative) lengths of the sections. For the slot arrangement shown in Fig. 2, with this approach we get $\rho_1=\rho_2=0.2$ and $\rho_3=0.6$.

4.2 Model with shear deformations

Flexural buckling of columns with considering the effect of in-plane shear deformations has been comprehensively studied in [47]. Various beam-like and shell-like models are considered, and analytical solutions are also derived in various options, including options that can (practically) precisely imitate constrained shell models such as the Ansys shell FE model or cFEM model used in this study. The critical force equation for this (termed as 'yny' option in [47]) option is as follows:

$$F_{cr}=\frac{F_a}{2F_{Fr}}\left\{F_{FS}\mp\sqrt{F_{FS}{}^2-\frac{4F_{Fr}}{F_a}\left[F_{Fr}F_S+\Delta F_F\left(F_{Fr}+F_S\right)\right]}\right\} \tag{18}$$

where

$$F_S=G\,A_S \tag{59}$$

$$\Delta F_F=F_F-F_{Fr}=\frac{\pi^2 E\left(I-I_r\right)}{\left(1-\nu^2\right)L^2} \tag{6}$$

$$F_{FS}=F_{Fr}\left(1+\frac{\Delta F_F}{F_a}\right)+F_S\left(1+\frac{F_{Fr}}{F_a}\right) \tag{21}$$

and G is the shear modulus, A_s is the shear area for the relevant direction. Obviously, the smallest critical force can be get by taking the negative sign in the formula. Furthermore, in case of thin-walled members, $\frac{\Delta F_F}{F_a}\cong 0$, therefore, F_{FS} in the critical force formula can be simplified to:

$$F_{FS}\cong F_{Fr}+F_S\left(1+\frac{F_{Fr}}{F_a}\right) \tag{22}$$

In the above formulae the F_s term is essentially the shear rigidity of the cross-section. If the web of the member is solid, the shear rigidity can be considered to be equal to the product of the web area and the shear modulus of elasticity. However, if the web is slotted, the definition of shear rigidity needs further considerations.

4.3 Equivalent shear rigidity of the web

Let us consider a web panel consisted of three parts with a reduced stiffness middle part, as shown in Fig. 10. We are searching for an equivalent shear modulus of the web panel so that the resultant shear deformations would be identical:

$$\frac{Vh}{G_{eq}}=\frac{V\,h_{u1}}{G_u}+\frac{V\,h_{u2}}{G_u}+\ldots+\frac{V\,h_{r1}}{G_r}+\frac{V\,h_{r2}}{G_r}+\ldots \tag{23}$$

where h_{u1}, h_{u2}, etc are the depths of the unslotted web parts, while h_{r1}, h_{r2}, etc. are the depths of those web parts where the shear rigidity is reduced due to the slots. Moreover, G_u is the shear modulus of the unslotted part, while G_r is the shear rigidity of the slotted part (and G_r should take account the effect of the holes and the effect of the shear deformations of the base material in the slotted web parts).

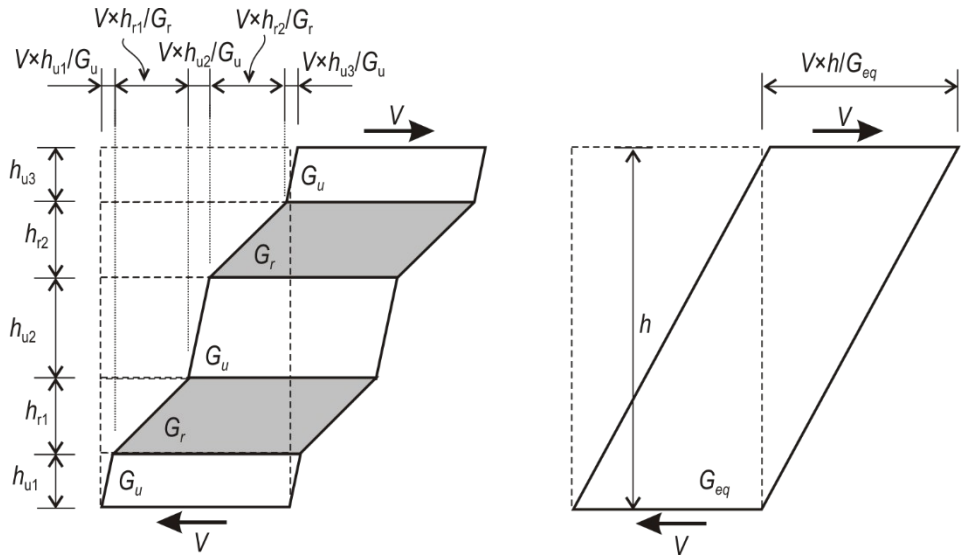

Figure 10: Equivalent shear rigidity interpretation

The above equation can also be written as:

$$\frac{Vh}{G_{eq}} = \frac{V\sum h_{u,i}}{G_u} + \frac{V\sum h_{r,j}}{G_r} \tag{24}$$

from which the equivalent shear rigidity can be expressed as:

$$G_{eq} = \frac{G_u G_r h}{G_u \sum h_{r,j} + G_r \sum h_{u,i}} \tag{25}$$

When the above model is applied to slotted webs, $\sum h_{r,j}$ is simply the total depth of the slotted parts, while $\sum h_{u,i}$ is the total depth of the unslotted part.

In Section 3.4 two ways are considered for the consideration of shear deformations: partial and full. When the above analytical model is applied to cases with allowing partial shear deformations, the shear deformations of the steel material is disregarded, therefore $G_u \to \infty$, thus the above formula can be simplified to:

$$G_{eq} = \frac{G_r h}{\sum h_{r,j}} \tag{26}$$

When the above analytical model is applied to cases with allowing full shear deformations, the shear rigidity of the steel material should be considered for the unslotted parts, therefore:

$$G_{eq} = \frac{G G_r h}{G \sum h_{r,j} + G_r \sum h_{u,i}} \tag{27}$$

In both the above cases we need the shear rigidity of the slotted parts, which can be determined by numerical or real experiments.

4.4 Shear rigidity of the slotted part of the web

To calculate the shear rigidity of the slotted web part, slotted panels have been analysed by shell FEM, using linear elastic analysis. The equivalent shear modulus is highly dependent on the number of slot rows and the length of the panel, but also influenced by many factors, such as

how exactly the shear load is applied, how the plate is supported, how the shear strain is interpreted.

Here the numerical results are shown for the following case: the slotted part is included in the model, but narrow, relatively rigid strips are attached (intended to represent the non-slotted parts of the profile), the edges are simply supported, the load is transferred along the longitudinal edges as uniformly distributed shear loads, the average shear strain is calculated as the average longitudinal translation of the longitudinal edges divided by the plate depth.

The tendencies are shown in Table 4. In Fig. 11 two deformed panels are presented for the full and partial shear cases, respectively. It is to observe that global shear-like deformations are obtained even in the partial shear option, due to the bending deformations of the small steel strips between the slots. However, the shear-like deformations are significantly larger if shear strains are allowed in the base material, too.

Table 4: Shear rigidity of the slotted panel, compared to G

length (mm)	shear	0 slot row	1 slot row	3 slot rows	5 slot rows	7 slot rows	11 slot rows	15 slot rows
500	full	1.00	0.29	0.19	0.16	0.14	0.12	0.10
1000	full	1.00	0.24	0.13	0.11	0.10	0.08	0.08
1500	full	1.00	0.22	0.11	0.09	0.09	0.07	0.07
2000	full	1.00	0.22	0.10	0.09	0.08	0.07	0.06
3000	full	1.00	0.21	0.09	0.08	0.07	0.06	0.06
5000	full	1.00	0.21	0.08	0.07	0.07	0.06	0.06
500	partial	>1.0	>1.0	>1.0	1.01	0.58	0.30	0.20
1000	partial	>1.0	>1.0	>1.0	0.54	0.33	0.19	0.14
1500	partial	>1.0	>1.0	0.70	0.38	0.25	0.15	0.12
2000	partial	>1.0	>1.0	0.52	0.31	0.21	0.13	0.11
3000	partial	>1.0	>1.0	0.35	0.23	0.17	0.12	0.10
5000	partial	>1.0	>1.0	0.23	0.17	0.13	0.10	0.09

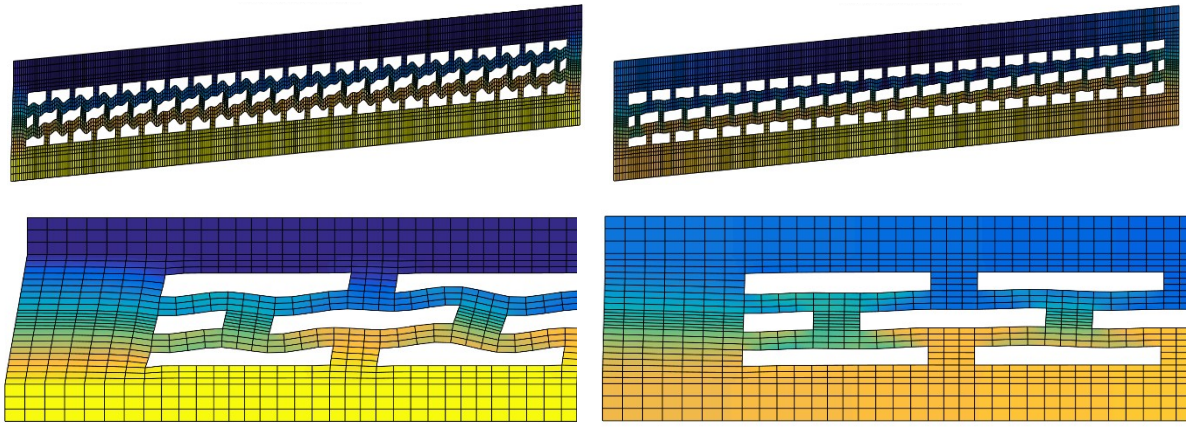

(a) full shear (b) partial shear

Figure 11: Deformations of a slotted panel in pure shear (enlarged by a factor of 4)

5 Numerical studies

5.1 Critical load comparison of cFEM and Ansys results

To compare the cFEM and Ansys calculations, a small parametric study has been performed, with 3 sections, 4 lengths, 3 shear options, 4 slot patterns. Some results are summarized in Table 5. As the numerical values prove, the differences are typically less than 1%. It is also to note that the calculations are relatively sensitive to the discretization, so it is reasonable to think that the experienced differences in critical loads are primarily due to the differences in the discretizations.

Table 5: Critical loads by Ansys, compared to cFEM results

FEM	section	shear	length (mm)	0 slot row	3 slot rows	5 slot rows	7 slot rows	
Ansys	C	full	500	14839	11173	9559	8155	kN
Ansys	C	full	1000	5684	4816	4334	3910	kN
Ansys	C	full	1500	2827	2565	2400	2249	kN
Ansys	C	full	2000	1658	1559	1491	1426	kN
cFEM	C	full	500	0.00	0.50	0.62	0.85	%
cFEM	C	full	1000	-0.03	0.46	0.68	1.47	%
cFEM	C	full	1500	-0.15	0.27	0.56	0.89	%
cFEM	C	full	2000	-0.02	0.19	0.55	0.65	%
Ansys	SA	partial	500	23330	20469	19113	17893	kN
Ansys	SA	partial	1000	6715	6197	5828	5486	kN
Ansys	SA	partial	1500	3063	2883	2753	2627	kN
Ansys	SA	partial	2000	1738	1679	1599	1537	kN
cFEM	SA	partial	500	-0.03	0.18	0.25	0.34	%
cFEM	SA	partial	1000	-0.34	-0.72	-0.58	-0.31	%
cFEM	SA	partial	1500	-0.15	0.07	0.14	0.21	%
cFEM	SA	partial	2000	-0.04	-1.14	0.02	0.03	%
Ansys	SS	no	500	23330	22104	21216	20222	kN
Ansys	SS	no	1000	6716	6392	6152	5853	kN
Ansys	SS	no	1500	3059	2912	2803	2678	kN
Ansys	SS	no	2000	1739	1657	1594	1538	kN
cFEM	SS	no	500	0.03	0.27	0.48	0.72	%
cFEM	SS	no	1000	-0.34	-0.34	-0.36	-0.03	%
cFEM	SS	no	1500	-0.02	0.02	0.02	-0.03	%
cFEM	SS	no	2000	-0.08	-0.12	-0.06	-1.08	%

5.2 Critical load comparison of cFEM and analytical results: without shear

For the considered slot geometries $\rho_1 = \rho_2 = 0.2$ and $\rho_3 = 0.6$ values have been applied,, as mentioned above. It is found that the coincidence between analytical and cFEM results is extremely good for any number of slot rows, as clearly shown by Table 6.

To illustrate the results of the analytical model (without considering in-plane shear deformations), Table 1 shows some critical forces calculated by cFEM, and the difference of the results from the analytical expression (with using $\rho_1=\rho_2=0.2$ and $\rho_3=0.6$ values). Only the results for C-sections are shown for a limited number of lengths, but the tendencies and observations are very similar for other (i.e., SA and SS) sections, too.

It can be observed that the analytical formula gives very precise estimation. Small differences exist if the column is very short, especially if there are many slot rows. The reason of the differences (most surely) is as follows: if the member is short, the behaviour is not totally uniform, e.g., at the ends there are no slots in the FE model, while the analytical model assumes a fully uniform rigidity distribution along the length. However, when the member is very short, the flexural buckling has little practical relevance. We can conclude, therefore, that the effect of holes is practically exactly assessed by the analytical model (without in-plane shear deformations) for members of realistic lengths.

Table 6: Critical loads, comparison of analytical results to cFEM results

FEM	section	length (mm)	0 slot row	3 slot rows	7 slot rows	11 slot rows	15 slot rows	
cFEM	C	500	23167	23069	22851	22331	21373	kN
cFEM	C	1000	6677.2	6659.8	6601.3	6460.3	6186.0	kN
cFEM	C	1500	3054.1	3049.6	3026.8	2964.7	2839.3	kN
cFEM	C	2000	1735.6	1733.8	1721.9	1687.2	1616.2	kN
cFEM	C	3000	777.11	776.56	771.56	756.31	724.56	kN
cFEM	C	5000	280.83	280.67	278.93	273.46	262.01	kN
Eq. (15)	C	500	0.00	-0.32	-0.89	-1.29	-1.49	%
Eq. (15)	C	1000	0.00	0.01	0.01	-0.01	0.01	%
Eq. (15)	C	1500	0.00	0.01	0.02	0.03	0.09	%
Eq. (15)	C	2000	0.00	0.00	0.01	0.02	0.09	%
Eq. (15)	C	3000	0.00	0.00	0.00	0.00	0.08	%
Eq. (15)	C	5000	0.00	0.00	-0.01	0.00	0.07	%

5.3 Critical load comparison of cFEM and analytical results: with partial shear

In Section 4.4 it is shown that the shear rigidity of the slotted part is significantly dependent on the member length and on the number of slot rows. However, from practical point of view the very short members have little importance (because very short members are not subjected to major-axis buckling). On the other hand, the shear deformations have little effect on long members. Moreover, it is impractical to use too small (e.g., 1 or 3) or too large (e.g., 11, 15) slot rows. It seems, therefore, to be sufficient to apply one single shear rigidity value, which well represents the practically more important cases. Based on the results of Table 7, this 'average' rigidity should be approx. 15-20% of the shear rigidity of the base material. Accordingly, the here presented numerical results assumes that the shear rigidity of the slotted web parts is 17% of the shear modulus of elasticity of the base material when shear deformations are partially allowed (i.e., when shear deformations are allowed in the holes excluded from the base material).

Table 7 shows results for SA-sections if the in-plane shear deformations are partially allowed (i.e, allowed in the slots, but not allowed in the steel material). The critical forces calculated by

cFEM, and the differences of the results from the analytical expressions are given. Only the results for SA-sections are shown, but the tendencies and observations are very similar for other (i.e., C and SS) sections, too.

The observation is that the analytical equation is reasonably precise. The tendency is as follows: the shorter the member and the more slot rows we have, the larger the difference between the cFEM and analytical results. However, if the member (for the actual, 200-mm-depth channel sections) is larger than 1000-1500 mm, the analytical formula is practically precise. For extremely short members the here-applied analytical calculation underestimates the critical load, which is primarily due to the underestimation of the equivalent shear rigidity. The analytical prediction could be improved by applying a problem-dependent shear rigidity of the slotted panels. Even though the difference can be relatively large, these extremely short lengths have little practical relevance (from the viewpoint of major-axis flexural buckling), therefore the application of one single equivalent shear rigidity for the slotted part (i.e., independently of the member length and of the number of rows) is practically sufficient.

Table 7: Critical loads, comparison of analytical results to cFEM results

FEM	section	length (mm)	0 slot row	1 slot rows	3 slot rows	5 slot rows	7 slot rows	
cFEM	SA	500	23336	22911	20507	19162	17955	kN
cFEM	SA	1000	6693.8	6618.4	6151.8	5794.0	5469.4	kN
cFEM	SA	1500	3058.5	3029.5	2885.0	2756.8	2632.7	kN
cFEM	SA	2000	1737.5	1722.2	1659.4	1599.1	1537.7	kN
cFEM	SA	3000	777.71	771.30	750.61	729.10	705.87	kN
cFEM	SA	5000	281.00	278.76	272.89	266.40	259.05	kN
Eq. (18)	SA	500	0.00	-4.75	-15.17	-25.18	-32.46	%
Eq. (18)	SA	1000	0.00	-1.60	-3.27	-5.72	-8.04	%
Eq. (18)	SA	1500	0.00	-0.75	-1.09	-1.78	-2.53	%
Eq. (18)	SA	2000	0.00	-0.43	-0.45	-0.65	-0.89	%
Eq. (18)	SA	3000	0.00	-0.19	-0.10	-0.04	0.00	%
Eq. (18)	SA	5000	0.00	-0.07	0.03	0.15	0.27	%

5.4 Critical load comparison of cFEM and analytical results: with full shear

In accordance with the findings of the previous Section, it seems to be sufficient to apply one single shear rigidity value for the slotted parts. Based on the results of Table 8, this ‘average’ rigidity should be approx. 7-8% of the shear rigidity of the base material if shear deformations are fully allowed. Accordingly, the here presented numerical results assume that the shear rigidity of the slotted web parts is 7.5% of the shear modulus of elasticity of the base material for the full shear deformations case (i.e., when shear deformations are due both to the holes and to shear deformations of the base material).

Sample results with fully allowing shear deformations are summarized in Table 8: critical forces calculated by cFEM, and the difference of the results from the analytical expression are given. Only the results for SS-sections are shown, but the tendencies and observations are very similar for other (i.e., C and SA) sections, too.

The observations w.r.t the full shear results are essentially identical to those mentioned at the partial shear results: for practical lengths the prediction of the analytical formula is reasonably

precise. The precision of the analytical prediction could be improved by applying a problem-dependent shear rigidity of the slotted panels, but this does not seem to be necessary.

Table 8: Critical loads, comparison of analytical results to cFEM results

FEM	section	length (mm)	0 slot row	2×1 slot rows	2×3 slot rows	2×5 slot rows	2×7 slot rows	
cFEM	SS	500	14449	12252	8630.2	6265.8	4462.4	kN
cFEM	SS	1000	5625.2	5177.7	4212.0	3439.9	2789.9	kN
cFEM	SS	1500	2809.2	2667.1	2331.8	2033.8	1760.2	kN
cFEM	SS	2000	1653.4	1591.8	1443.0	1303.1	1165.0	kN
cFEM	SS	3000	760.31	740.30	692.18	644.30	594.41	kN
cFEM	SS	5000	278.69	273.07	260.15	246.70	232.03	kN
Eq. (18)	SS	500	10.483	8.124	-8.919	-11.372	-4.049	%
Eq. (18)	SS	1000	4.054	3.959	-1.724	-2.653	0.343	%
Eq. (18)	SS	1500	2.024	2.214	-0.067	-0.356	1.305	%
Eq. (18)	SS	2000	1.192	1.395	0.354	0.333	1.650	%
Eq. (18)	SS	3000	0.546	0.722	0.585	0.865	1.780	%
Eq. (18)	SS	5000	0.199	0.345	0.593	1.004	1.705	%

6 Summary and conclusions

In this paper the major-axis elastic flexural buckling of channel members with slotted web is investigated. Channel members without and with a (centrally spaced) longitudinal stiffener are studied. The so-called constrained finite element method has been applied to identify those factors that influence the buckling behaviour. The results show that the notion of flexural buckling is not obvious as soon as the problem is solved by a shell model, such as a shell finite element analysis. In case of slotted web, the shear rigidity of the web is radically reduced, which, if the in-plane shear deformations are fully or partially allowed, has pronounced effect on the flexural buckling (both buckling shape and critical load). As numerical results show, the reduction of the shear rigidity of the slotted web is significantly dependent on the slot pattern and the member length. It has also been shown that the axial and bending rigidity of the member are reduced due to the slots, which might have a small, but sometimes non-negligible effect on the buckling.

An analytical model has been proposed to calculate the critical load for thin-walled members with slotted webs. The model is able to consider all the important effects, including the effect of longitudinal second-order strain terms (which is typically considered in shell models, but disregarded in most beam models), the degrading effect of the slots on the axial and bending rigidity, as well as the effect of in-plane shear deformations of the slotted web. Extended numerical studies have been conducted, covering a wide range of column lengths and slot geometries. The results of the numerical studies justify the applicability of the constrained finite element method, as well as show that the analytical model gives a reasonably precise prediction for the critical loads.

In this paper major-axis flexural buckling is discussed only. It is believed, however, that the effect of slots to other types of global buckling are similar, therefore, the conclusions drawn here would qualitatively be valid for other types of global buckling. This question, i.e., other types of global buckling, might be the topic of future papers.

Acknowledgements

The presented work was conducted with the financial support of the K119440 project of the Hungarian National Research, Development and Innovation Office.

References

[1] Sweedan A.M.I, El-Sawy K.M, Elastic local buckling of perforated webs of steel cellular beam–column elements, *Journal of Constructional Steel Research*, 67(7), pp. 1115-1127, 2011.

[2] Gu J., Cheng S., Shear effect on buckling of cellular columns subjected to axially compressed load, *Thin-Walled Structures*, Vol 98, Part B, pp. 416-420, 2016.

[3] Pham C.H., Shear buckling of plates and thin-walled channel sections with holes, *Journal of Constructional Steel Research*, Vol 128, pp. 800-811, 2017.

[4] Yuan W., Yu N., Li L., Distortional buckling of perforated cold-formed steel channel-section beams with circular holes in web, *International Journal of Mechanical Sciences*, Vol 126, pp. 255-260, 2017.

[5] Horáček M., Melcher J., Pešek O., Brodniansky L., Focusing on Problem of Lateral Torsional Buckling of Beams with Web Holes, *Procedia Engineering*, Vol 161, pp. 549-555, 2016.

[6] Moen C.D., Schafer B.W., Experiments on cold-formed steel columns with holes, *Thin-Walled Structures*, 46(10), pp. 1164-1182, 2008.

[7] Yingjiang Z., Renjun Y., Hongxu W., Experimental and numerical investigations on plate girders with perforated web under axial compression and bending moment, *Thin-Walled Structures*, Vol 97, pp. 199-206, 2015.

[8] Yao Z., Rasmussen K.J.R., Inelastic local buckling behaviour of perforated plates and sections under compression, *Thin-Walled Structures*, Vol 61, pp. 49-70, 2012.

[9] Brando G., De Matteis G., Buckling resistance of perforated steel angle members, *Journal of Constructional Steel Research*, Vol 81, pp. 52-61, 2013.

[10] Gunawan D., Suryoatmono B., Numerical Study on Lateral-torsional Buckling of Honeycomb Beam, *Procedia Engineering*, Vol 171, pp. 140-146, 2017.

[11] Yao Z., Rasmussen K.J.R., Material and geometric nonlinear isoparametric spline finite strip analysis of perforated thin-walled steel structures - analytical developments, *Thin-Walled Structures*, Vol 49, pp. 1359-1373, 2011.

[12] Yao Z., Rasmussen K.J.R., Material and geometric nonlinear isoparametric spline finite strip analysis of perforated thin-walled steel structures – numerical investigations, *Thin-Walled Structures*, Vol 49, pp. 1374-1391, 2011.

[13] Moen C.D., Schafer B.W., Elastic buckling of cold-formed steel columns and beams with holes, *Engineering Structures*, 31(12), pp. 2812-2824, 2009.

[14] Casafont M., Pastor M., Bonada J., Roure F., Peköz T., Linear buckling analysis of perforated steel storage rack columns with the Finite Strip Method, *Thin-Walled Structures*, Vol 61, pp. 71-85, 2012.

[15] Smith F.H, Moen C.D., Finite strip elastic buckling solutions for thin-walled metal columns with perforation patterns, *Thin-Walled Structures*, Vol 79, pp. 187-201, 2014.

[16] Silvestre N., Camotim D., Silva N.F., Generalized Beam Theory revisited: from the kinematical assumptions to the deformation mode determination, *Int. Journal of Structural Stability and Dynamics*, 11(5), pp. 969-997, 2011.

[17] Bebiano R., Gonçalves R., Camotim D., A cross-section analysis procedure to rationalise and automate the performance of GBT-based structural analyses, *Thin-Walled Structures*, Vol 92, pp. 29-47, 2015.
[18] Ádány S., Schafer B.W., Buckling mode decomposition of single-branched open cross-section members via Finite Strip Method: derivation, *Thin-Walled Structures* **44**(5), pp. 563-584, 2006.
[19] Ádány S., Schafer B.W., Buckling mode decomposition of single-branched open cross-section members via Finite Strip Method: application and examples, *Thin-Walled Structures*, **44**(5), pp. 585-600, 2006.
[20] Ádány S., Schafer B.W., A full modal decomposition of thin-walled, single-branched open cross-section members via the constrained finite strip method, *Journal of Constructional Steel Research*, 64 (1), pp. 12-29, 2008.
[21] Ádány S., Schafer B.W., Generalized constrained finite strip method for thin-walled members with arbitrary cross-section: Primary modes, *Thin-Walled Structures*, Vol 84, pp. 150-169. 2014.
[22] Ádány S., Schafer B.W., Generalized constrained finite strip method for thin-walled members with arbitrary cross-section: Secondary modes, orthogonality, examples, *Thin-Walled Structures*, Vol 84, pp. 123-133. 2014.
[23] Nedelcu M., GBT-based buckling mode decomposition from finite element analysis of thin-walled members, *Thin-Walled Structures*, vol. 54, pp. 156-163, 2012.
[24] Casafont M., Marimon F., Pastor M.M., Calculation of pure distortional elastic buckling loads of members subjected to compression via the finite element method, *Thin-Walled Structures*, 47(6-7), pp. 701-72, 2009.
[25] Casafont M., Marimon F., Pastor M.M., Ferrer M., Linear buckling analysis of thin-walled members combining the Generalised Beam Theory and the Finite Element Method, *Computers and Structures*, 89(21-22), pp. 1982-2000, 2011.
[26] Cai J., Moen C.D., Elastic buckling analysis of thin-walled structural members with rectangular holes using generalized beam theory, *Thin-Walled Structures*, Vol 107, pp. 274-286, 2016.
[27] Casafont M., Bonada J., Pastor M.M. and Roure F. GBT calculation of distortional and global buckling of cold-formed steel channel columns with multiple perforations, Eighth International Conference on Advances in Steel Structures, Lisbon, Portugal, July 22-24, 2015, paper no:87, p. 18.
[28] Casafont M., Bonada J., Pastor M.M. and Roure F. GBT calculation on elastic buckling loads of cold-formed steel rack columns, *Proceedings* of the International Colloquium on Stability and Ductility of Steel Structures, SDSS 2016, (eds. D. Dubina, V. Ungureanu), Timisoara, Romania, May 30 – June 1, 2016, pp. 297-304.
[29] ANSYS, Inc. ANSYS ®Mechanical, Release 17.1.
[30] Ádány S., Shell element for constrained finite element analysis of thin-walled structural members, *Thin-Walled Structures*, Volume 105, August 2016, Pages 135-146.
[31] Visy D., Ádány S., Local elastic and geometric stiffness matrices for the shell element applied in cFEM, submitted to *Periodica Polytechnica ser. Civil Engineering*
[32] Ádány S., Constrained shell Finite Element Method for thin-walled members, Part1: constraints for a single band of finite elements, *Thin-Walled Structures*, Vol 128, July 2018, pp. 43-55. doi:10.1016/j.tws.2017.01.015
[33] Ádány S, Visy D, Nagy R: Constrained shell Finite Element Method, Part 2: application to linear buckling analysis of thin-walled members, *Thin-Walled Structures*, Vol 128, July 2018, pp. 56-70. doi:10.1016/j.tws.2017.01.022
[34] Ádány S.: Constrained shell Finite Element Method for thin-walled members with holes, *Thin-Walled Structures*, vol 121, pp. 41-56. (2017)

[35] Höglund T., Burstrand H.: Slotted steel studs to reduce thermal bridges in insulated walls, *Thin-Walled Structures*, Vol 32(1–3), 1998, pp. 81-109. doi.org/10.1016/S0263-8231(98)00028-7
[36] Restrepo J.I, Bersofsky A.M, Performance characteristics of light gage steel stud partition walls, *Thin-Walled Structures*, Vol 49(2), 2011, Pages 317-324, doi.org/10.1016/j.tws.2010.10.001
[37] Ma Q., Wang P., Simplified stability design method for the stiffened plate with slotted holes under uniform compression, *Thin-Walled Structures*, Vol 68, 2013, pp. 35-41, doi.org/10.1016/j.tws.2013.02.017
[38] Degtyarev N.V, Degtyareva V.V., Experimental investigation of cold-formed steel channels with slotted webs in shear, *Thin-Walled Structures*, Vol 102, 2016, pp. 30-42, doi.org/10.1016/j.tws.2016.01.012
[39] Degtyarev V.V, Degtyareva N.V., Finite element modeling of cold-formed steel channels with solid and slotted webs in shear, *Thin-Walled Structures*, Vol 103, 2016, pp. 183-198, doi.org/10.1016/j.tws.2016.02.016.
[40] Degtyarev V.V, Degtyareva N.V., Numerical simulations on cold-formed steel channels with flat slotted webs in shear. Part I: Elastic shear buckling characteristics, *Thin-Walled Structures*, Vol 119, 2017, pp. 22-32, doi.org/10.1016/j.tws.2017.05.026.
[41] Degtyarev V.V, Degtyareva N.V., Numerical simulations on cold-formed steel channels with flat slotted webs in shear. Part II: Ultimate shear strength, *Thin-Walled Structures*, Vol 119, 2017, pp. 211-223, doi.org/10.1016/j.tws.2017.05.028.
[42] Degtyarev V.V, Degtyareva N.V., Numerical simulations on cold-formed steel channels with longitudinally stiffened slotted webs in shear, *Thin-Walled Structures*, Vol 129, 2018, pp. 429-456. https://doi.org/10.1016/j.tws.2018.05.001.
[43] Degtyareva N.V., Review of Experimental Studies of Cold-Formed Steel Channels with Slotted Webs under Bending, *Procedia Engineering*, Vol 206, 2017, pp. 875-880, doi.org/10.1016/j.proeng.2017.10.566.
[44] Geleji B., Szedlák M., Visy D., Ádány S., „Understanding the global buckling behaviour of thin-walled members with slotted web", *Proceedings* of the 22nd International Speciality Conference on Cold-Formed Steel Structures, Nov 5-6, 2014, St. Louis, USA (eds: R.A. LaBoube, W.W. Yu), pp. 51-66.
[45] Ádány S., Visy D.: Global Buckling of Thin-Walled Columns: Numerical Studies, *Thin-Walled Structures* Vol 54, 2012, pp. 82-93.
[46] Ádány S.: Global Buckling of Thin-Walled Columns: Analytical Solutions based on Shell Model, *Thin-Walled Structures* (2012), Vol 55, pp 64-75. doi:10.1016/j.tws.2012.02.002
[47] Ádány S.: Flexural Buckling of Simply Supported Thin-Walled Columns with Consideration of Membrane Shear Deformations: Analytical Solutions based on Shell Model, *Thin-Walled Structures,* Vol 74, pp. 36-48, 2014.